Aeroacoustic calculations of a full scale Nordtank 500kW wind turbine

Debertshäuser, Harald; Shen, Wen Zhong; Zhu, Wei Jun

Published in:
Journal of Physics: Conference Series (Online)

Link to article, DOI:
10.1088/1742-6596/753/2/022032

Publication date:
2016

Document Version
Publisher's PDF, also known as Version of record

Aeroacoustic calculations of a full scale Nordtank 500kW wind turbine

2016 J. Phys.: Conf. Ser. 753 022032

(http://iopscience.iop.org/1742-6596/753/2/022032)

Aeroacoustic calculations of a full scale Nordtank 500kW wind turbine

H Debertshäuser, W Z Shen and W J Zhu
Nils Koppels Allé, Building 403, 2800 Kgs. Lyngby

E-mail: hadeb@dtu.dk

Abstract. The Actuator Line/ Navier-stokes technique is used to compute the incompressible flow around a full scale Nordtank 500kW wind turbine under different complex flow conditions such as atmospheric turbulence and wind shear. The flow field is used as an input to aeroacoustic calculations based on; a semi empirical noise model; and a Navier-Stokes based computational aeroacoustic code (CAA). The Navier-Stokes based approach is solving acoustic perturbation equations and is capable of taking propagation and ground effects into account, but is limited to low frequency noise due to feasible mesh resolution, and due to the simplification in the actuator line method using body forces to represent the blade. Noise levels are compared to field measurements of a Nordtank 500kW wind turbine at different wind speeds and inflow profiles.

1. Introduction

Wind turbine noise has been identified by Megavind, a strategic partnership for the Danish wind industry, as the most important environmental impact of wind-energy systems [1]. The pace of growth of on-shore wind energy has led to turbines being placed closer to where people live. Placing the turbines close to residential areas creates social acceptance problems, especially in densely populated areas such as Europe. Consequently noise regulations have become stricter, particularly in Denmark.

In the past decades mechanical noise has been a major issue, but due to improved components designs this has been lowered significantly. Therefore the focus is now on aerodynamic generated noise.

Aeroacoustic noise can be divided into two major mechanisms: airfoil self-noise, and turbulent inflow noise. Turbulent inflow noise appears due to the interaction of incoming turbulent eddies in the atmospheric boundary layer with the blade. These eddies are rather big in comparison to the size of eddies in the boundary layer developing along the blade surface. Because of that turbulent inflow noise is the dominant noise source at lower frequencies. Airfoil self-noise is generated by of the boundary layer interaction on the pressure and suction side at the trailing edge. Vortices in the boundary layer on the pressure and suctiion side interact with the hard blade surface, especially at the sharp trailing edge, radiating acoustic waves. Since the boundary layer is relatively thin, the main contribution of airfoil self-noise is at higher frequencies.

The flow around a single wind turbine or a wind farm is very complex due to wind shear, yaw, atmospheric turbulence, and wake effects. Hence it is important to have high fidelity codes for the flow and the acoustics to be able to capture these flow conditions and their effect on wind turbine noise.

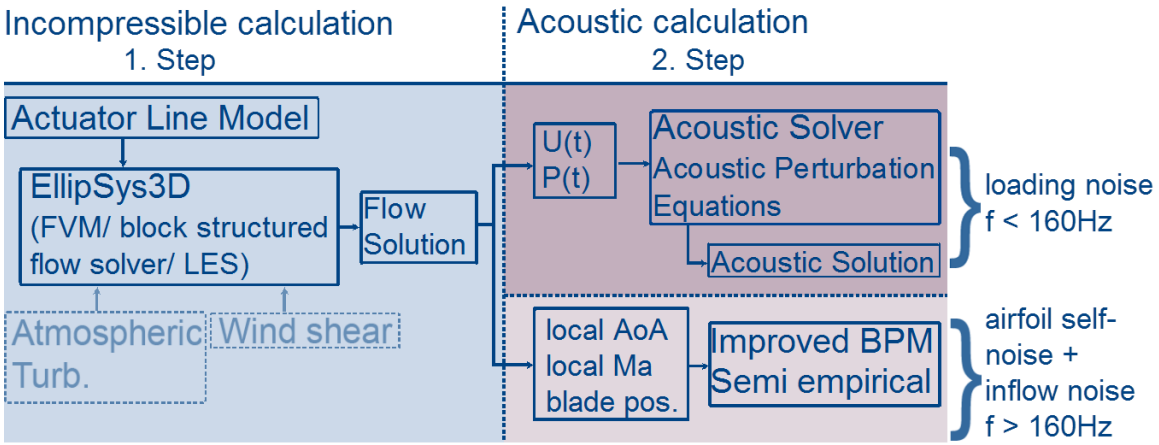

Figure 1. Flow chart of the used methodology

2. Methodology

A two-step approach is used to calculate aerodynamic noise of a wind turbine. The flow chart in Figure 1 gives an overview of the methodology.

First the flow field around a wind turbine is simulated using Large Eddy Simulation (LES) with the Finite Volume Method, block structured, multi grid solver EllipSys3D, developed at Denmark Technical University [2] with the actuator line method [3]. In a second step the acoustic calculations are done based on the flow simulation as input. For the acoustic calculation two different methods are used, an acoustic model based on semi empirical scaling laws, and a high fidelity model based on solving the Navier-Stokes equations.

2.1. Actuator Line Technique

In the actuator line method forces mimicking the wind turbine blades are added by introducing additional source terms to the Navier-Stokes equations,

$$\frac{\partial U_i}{\partial t} + \frac{\partial (U_i U_j)}{\partial x_j} = -\frac{1}{\rho_0}\frac{\partial P}{\partial x_i} + \nu \frac{\partial^2 U_i}{\partial x_j^2} + f_i \tag{1}$$

$$\frac{\partial U_i}{\partial x_i} = 0 \tag{2}$$

$$f_{2D} = \frac{1}{2}\rho U_{rel}^2 c(C_l e_l + C_d e_d) \tag{3}$$

with U_i as velocity, P as incompressible pressure, ρ as density, ν as kinematic viscosity, c as chord length, $C_l(\alpha, Re)$ and $C_d(\alpha, Re)$ as lift and drag coefficient, f_i as the added body forces, f_{2D} as the force per spanwise unit length, and U_{rel} as the local relative flow velocity close to the blade segment. The forces f_{2D} are calculated using tabulated airfoil data and are then introduced as smeared body forces f_i in the Navier-Stokes equations. Turbulent stresses are modelled by the mixed-scale turbulence model of Ta Phuoc [4].

Different flow conditions can be added to the flow simulation, such as wind shear , and atmospheric turbulence. Wind shear follows equation (4),

$$U = U_\infty (\frac{y}{H})^\alpha \tag{4}$$

with U_∞ as a reference wind speed at a specified height H and a shear exponent α.
Atmospheric turbulence is introduced with a Mann box [5]. The Mann model assumes a constant shear based on a roughness length z_0. Body forces are added in the flow calculations at a slice upstream the wind turbine, creating a velocity field with atmospheric turbulence.

2.2. Acoustic perturbation equations
To take propagation and ground effects into account and to study the development of aeroacoustic noise in the source region a high fidelity method is needed. A Navier-Stokes based approach, the acoustic splitting technique, developed by Shen and Sørensen [6] is used to capture those effects. The acoustic calculation is split into two steps: solving the incompressible flow field, and solving acoustic perturbation equations (5-8). The acoustic perturbation equations are derived by introducing the compressible flow variables with a decomposition of an incompressible and an acoustic part.

$$u_i = U_i + u_i', \quad p = P + p', \quad \rho = \rho_0 + \rho', \quad g_i = \rho u_i + \rho' U_i \tag{5}$$

$$\frac{\partial \rho'}{\partial t} + \frac{\partial g_i}{\partial x_i} = 0 \tag{6}$$

$$\frac{\partial g_i}{\partial t} + \frac{\partial}{x_j}[g_i(U_j + u_j') + \rho_0 U_i u_j' + p'\delta_{ij}] = \frac{\partial \tau_{ij}'}{\partial x_j}, \quad \tau_{ij}' = \mu(\frac{\partial u_i'}{\partial x_j} + \frac{\partial u_j'}{\partial x_i} - \frac{2}{3}\delta_{ij}\frac{\partial u_k'}{\partial x_k}) \tag{7}$$

$$\frac{\partial p'}{\partial t} - c^2\frac{\partial \rho'}{\partial t} = -\frac{\partial P}{\partial t}, \quad c^2 = \frac{\gamma p}{\rho} = \frac{\gamma(P+p')}{\rho_0 + \rho'} \tag{8}$$

Instantaneous incompressible velocities U_i and pressure P are taken from the incompressible LES computation.
The main source term in these equations is the fluctuating incompressible pressure $\frac{\partial P}{\partial t}$. With this splitting it is possible to use different meshes for flow and acoustic simulation and to use different time steps for both calculations. Using different time steps is especially beneficial in low Mach number flows.

2.3. Improved Brooks, Pope, Marcolini model
Based on experimental data and acoustic scaling laws semi empirical acoustic formulas for airfoils were developed by Brook, Pope, and Marcolini [7] and by Lowson [8]. Those semi empirical noise models have been combined and extended to wind turbine level by Zhu et al. [9]-[10] in the Improved Brooks, Pope, Marcolini (IBPM) model, which takes into account the detailed blade shapes and the consideration of trailing edge shapes in the new blunt trailing edge noise model. In Figure 2 sketches of airfoil self noise mechanisms are shown (left), and the methodology of the IBPM model (right). The blade is divided into airfoil sections. At each section the noise of an airfoil is calculated based on local angle of attack, and local relative flow velocity. Those quantities are input from the incompressible flow solution at each time step. The noise levels for each airfoil segment at each blade are summed up in 1/3 octave band with respect to a specified observer position. Due to the input of the incompressible LES actuator line model computation, noise calculations can be done for any flow condition around the wind turbine, such as atmospheric turbulence, and wind shear.

3. Results
Aeroacoustic calculations are done for a Nordtank 500kW wind turbine with a blade radius of $R = 20.5m$ and a hub height of $H = 1.8R = 36m$. The computations are compared to

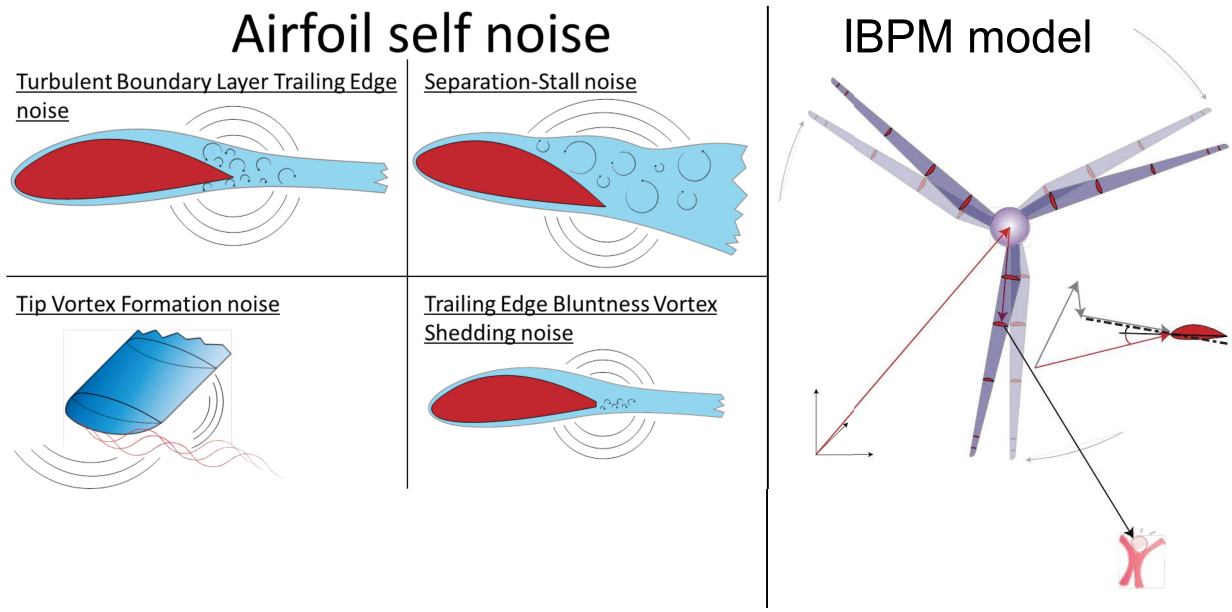

Figure 2. (left)Sketch of airfoil self noise mechanisms; (right) methodology of the IBPM model

measurements. Details about the measurements can be found in [11]. Hence the numerical setup is chosen to match the wind conditions of the measurement day. The incoming wind profile during the measurements was fitted to a logarithmic velocity profile, leading to an estimated roughness height of $z_0 = 0.1m$. In the present calculations a wind shear profile is used. The logarithmic and wind shear profile is matched at hub height, resulting in a wind shear factor of

$$\alpha = \frac{1}{ln(z_{ref}/z_0)} = 0.17. \tag{9}$$

The tip speed ratio is set to $\lambda = 10, 7.5, 6.0$ leading to a wind speed of $6, 8$, and $10m/s$ at hub height. Atmospheric turbulence is introduced by a Mann box at a distance of $6R$ in front of the wind turbine. For each wind speed a turbulent box was created, with a surface roughness of $z_0 = 0.1m$. The average turbulent intensity is about 11% in the stream-wise direction for all three boxes. 9% is reported for the measurements. The Mann box has a dimension of $[12R; 12R; 380R]$.

3.1. Actuator line solution

In Figure 3 the stream-wise velocity field for a wind speed of $10m/s$ is shown. The wind turbine is placed at $Z = 5R; Y = 1.8R$, and its position is indicated as a black vertical line. Atmospheric turbulence is introduced at $Z = -1R$ and has a significant influence on the incoming flow facing the wind turbine, as well as on the wake development. In particular it has an influence on local angel of attack and local relative velocity, that are inputs to the semi empirical noise calculation. To validate the loading, integral values are compared against measurements. In Figure 4 thrust coefficient $C_T = \frac{T}{1/2\rho AV^2}$, and power coefficient $C_P = \frac{P}{1/2\rho AV^3}$ are compared against measured values [12]. The agreement is fairly good. The slope of C_T curve is slightly higher than the measured one, with a maximum difference $\Delta C_T = 0.05$. The shape of the power coefficient is matched, with a peak at $v = 8m/s$ or a tip speed ratio of $\lambda = 7.5$. The maximum deviation ΔC_P

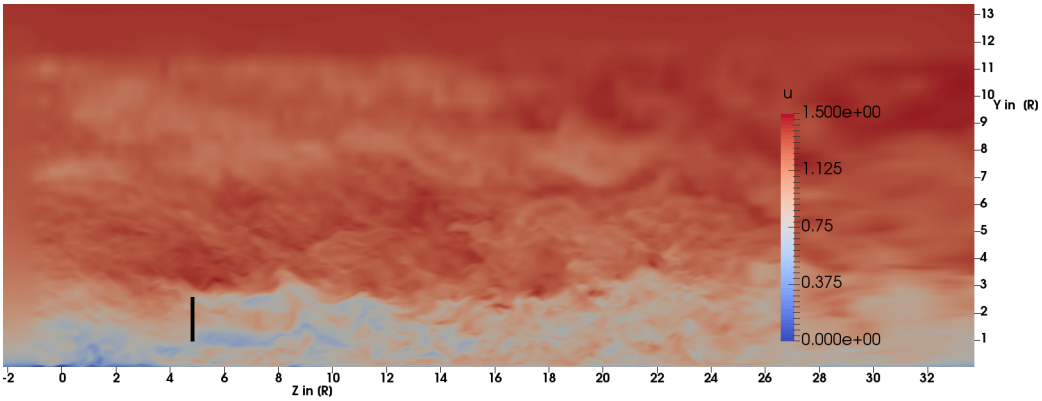

Figure 3. Steam-wise velocity field out of actuator line method; turbine is placed at $z = 5R, y = 1.8R$; black line indicates position of the wind turbine; $u = 1$ corresponds to $10m/s$

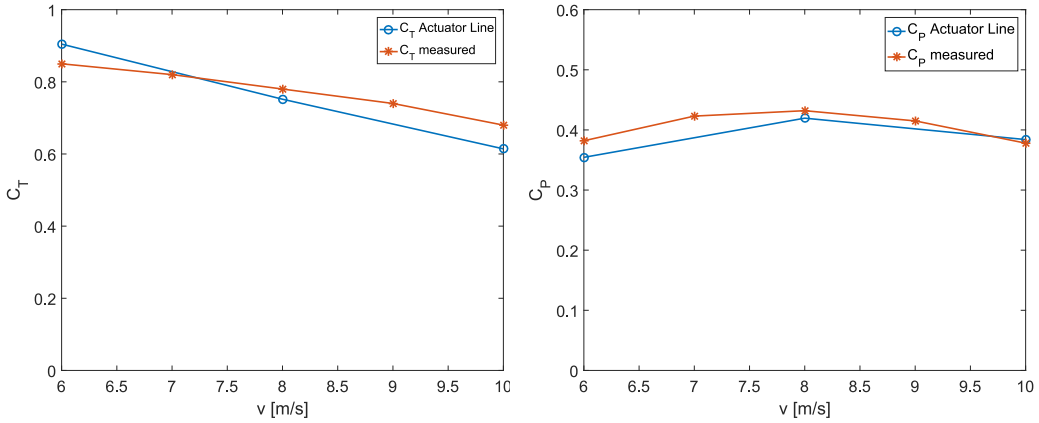

Figure 4. C_T and C_P values out of measurements [12] compared to calculated values out of actuator line simulations

is 0.025. From this we conclude that the integral forces applied are correct for the considered cases.

The local forces along the blades cause a fluctuating incompressible pressure $\frac{\partial P}{\partial t}$ that acts as a source term in the acoustic perturbation equations and can be seen in Figure 5. On the left (a) the local normalized forces at selected span wise sections are shown. They are oscillating with blade passing frequency, but have a superposed fluctuation due to the atmospheric turbulence. The loading is highest at the outer part of the blade and so are the force fluctuations. From this it can be expected that the acoustic sources are strongest in the outer part of the blade. On the right (b) the power spectral density (PSD) of the normalized forces are plotted. The highest spectral energy is in the lower frequencies and decays to higher frequencies. The sampling frequency is $300Hz$.

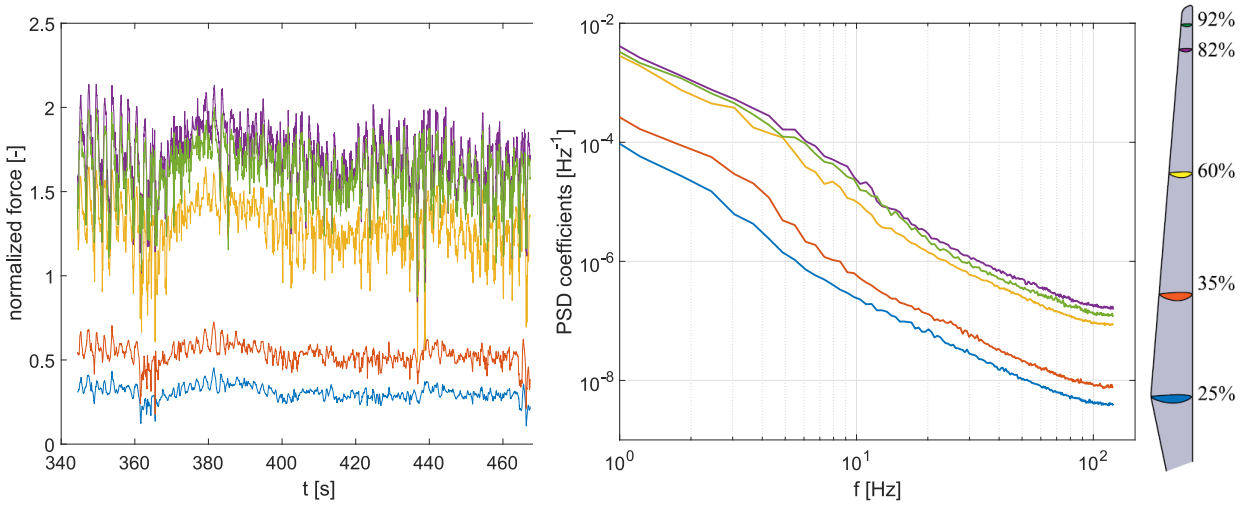

Figure 5. (a) Normalized forces along span over time; (b) Power spectral density of normalized forces

3.2. Acoustic Perturbation Equation

As mentioned in the last section the forces on the blade generate a pressure change with respect to time $\frac{\partial P}{\partial t}$. This acts as a source term in equation (8) leading to an acoustic pressure change. The instantaneous acoustic pressure field due to the wind turbine can be seen in Figure 6 for a wind speed of $10m/s$. Acoustic waves are formed by the blades and propagate away from the wind turbine. The blade position of one blade is at an azimuthal angle of 180%, which corresponds to the blade being in the plane plotted, at bottom position. The highest instantaneous acoustic pressure is at the outboard section of the plane, since the aerodynamic forces are highest in this region (see Figure 5) and almost no noise is generated at the root part of the blade. Atmospheric turbulence adds fluctuations to the acoustic waves, that are modulated on a acoustic pressure change with the blade passing frequency.

The influence of the ground can also be seen. An acoustically hard wall has been set, so that acoustic waves hitting the ground are fully reflected.

In Figure 7 the narrowband sound pressure level at a position $2.2R$ downstream of the turbine is compared to data from measurements for wind speeds of $v = 6, 8, 10m/s$. The grey solid lines are measurements data with the turbine in operation, the grey dashed lines are background noise measurements data with the turbine turned off. The coloured solid lines represent the acoustic pressure calculated with the acoustic perturbation equations.

The comparison shows a mismatch between the spectrum of the acoustic pressure with the spectrum from the measurements. The sound pressure level decays too fast for frequencies above $10Hz$. We conclude that this is due to the fact, that the geometry of the blades as solid walls and the boundary layers of the blades are not resolved in the actuator line method. The mechanism of small turbulent eddies in the boundary layer interacting with the solid blade generating aerodynamic noise is not captured by modelling the blades with the actuator line technique. In future work additional noise sources out of the semi empirical IBPM model will be introduced along the blades in the acoustic perturbation equations to capture this.

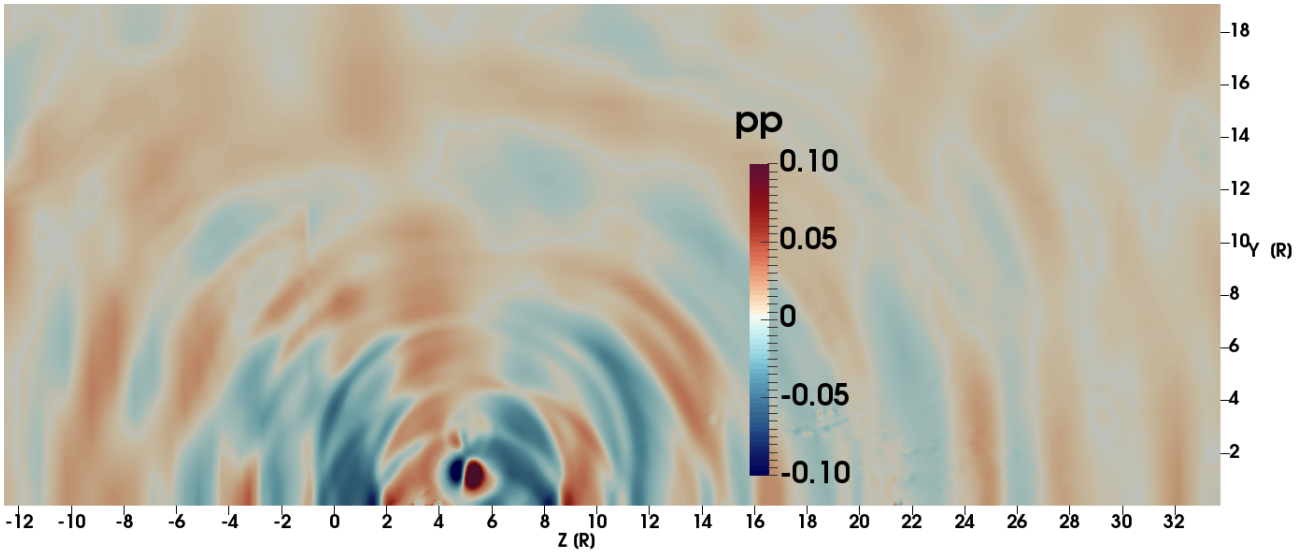

Figure 6. Acoustic pressure out of acoustic perturbation equation calculation for wind speed of 10m/s; Turbine is placed at $Z = 5R; Y = 1.8R$

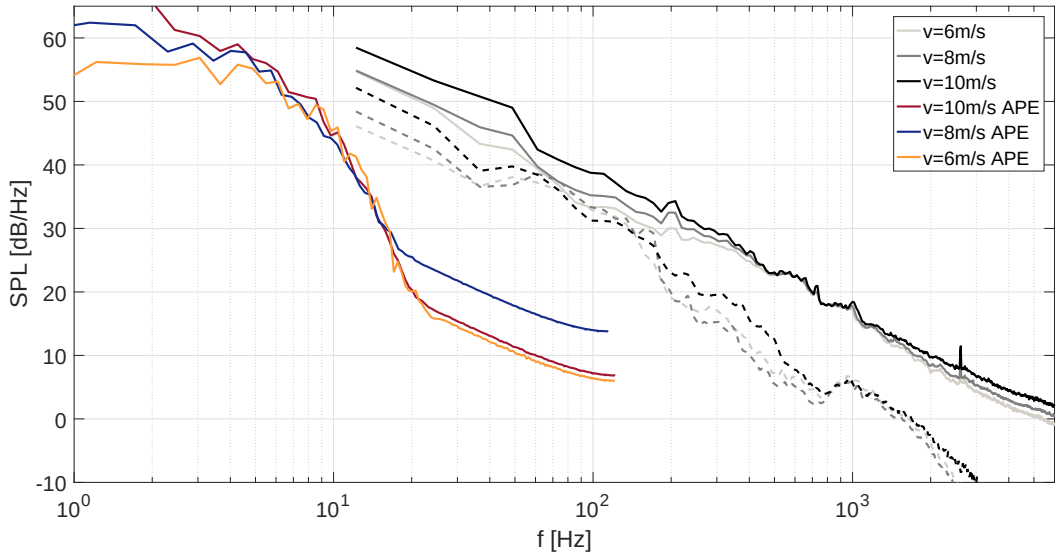

Figure 7. Comparison of narrow band acoustic pressure out of acoustic perturbation equation calculations at $2.2R$ behind the turbine with narrow band measurement results at wind speeds of $v = 6, 8, 10m/s$; dashed lines indicate back ground noise

3.3. IBPM

In Figure 8 the calculated A-weighted sound pressure level at $45m$ behind the wind turbine and ground level can be seen for wind speeds of $6, 8, and 10m/s$ for a $2min$ period. The sound pressure level changes periodically with the blade passing frequency and is about $2dB(A)$. This is usually referred as amplitude modulation noise (AM). Atmospheric turbulence adds fluctuations to the local angle of attack, and directivity. Due to the random appearance of the none-periodic change in sound pressure level people are usually more annoyed by the perceived sound. Hence being able to calculate this contribution is important for wind turbine noise prediction tools.

In Figure 9 A-weighted sound pressure level in 1/3 octave bands out of the semi empirical model improved BPM model is compared to data from measurements. A comparison with the microphone in downwind position is shown. The semi empirical noise model is in good agreement with the experiment, especially for wind speeds of $8m/s$ and $10m/s$. The peak in the experiments at ca. $50Hz$ is due to mechanical noise and cannot be captured with the aeroacoustic noise model. Background noise has been added to the computations to make a fairer comparison to the experimental data. As can be seen in Figure 7 the background noise is almost as high as the wind turbine noise between $60 - 160Hz$. For $10m/s$ the calculated noise level show for frequencies below $200Hz$ up to $4dB$ deviation to the measurements. In this range the wind turbine noise is dominated by turbulent inflow noise. One explanation is, that a fixed value of 11% turbulence intensity is used in the model for the turbulent inflow noise. These 11% are the mean turbulent intensity of the Mann box. Due to the shear turbulent intensity varies with height and is higher at lower levels above ground and hence TI noise levels could be under predicted.

At frequencies above $5kHz$ the IBPM model over predicts the noise levels for wind speeds of $6m/s$ and $8m/s$. In this region trailing edge bluntness noise dominates. This behavior has been observed before and a new bluntness model was recently published [10].

Highest A-weighted sound pressure level of ca. $40dB(A)$ appear at $600Hz$. The semi empirical noise model predicts lower levels at lower wind speeds. The measurements almost collapse at this frequency, while usually a decrease in sound pressure levels is seen for lower wind speeds. Overall the semi empirical noise model predicts the sound pressure levels of the Nordtank 500kW wind turbine well.

4. Conclusions

Aerodynamic noise computations of a full scale Nordtank 500kW for wind speeds of $6, 8$, and $10m/s$ were presented. Two methods are used to compute the noise: a Navier-Stokes based approach solving acoustic perturbation equations; and a semi empirical noise model. With the acoustic perturbation calculation ground, and propagation effects are included. Acoustic pressure is calculated in the whole domain and hence it is possible to get the acoustic response as a 3D field. An acoustical hard surface was used, and the influence of it was shown in a slice, cut through the wind turbine origin in the stream-wise direction. Compared to measurements the spectrum of the acoustic pressure at $45m$ behind the turbine at ground level shows a mismatch in amplitude for frequency above $10Hz$.

In the flow computation, that is used as an input for the acoustic perturbation equation calculation, the blade is modelled with body forces in the actuator line technique. Hence the blade geometry and the boundary layers of the blades are not resolved. Noise due to the interaction of the blade geometry and the boundary layer is not fully captured. In future work the semi empirical IBPM noise model will be used to introduce additional noise sources in the acoustic perturbation equations along the blade to capture noise at higher frequencies.

The comparison with the semi empirical noise model shows good agreement. It could be shown that OAM appears due to the atmospheric boundary layer and its effect on change in local angle of attack and relative flow velocity. Sound pressure levels in 1/3 octave bands fit well with the

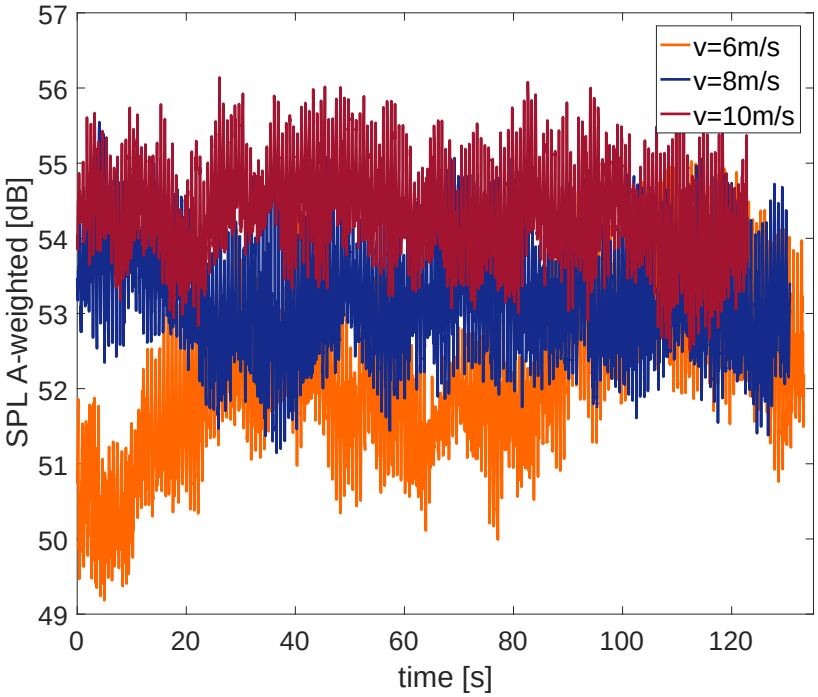

Figure 8. A-weighted sound pressure levels for wind speeds of $v = 6, 8, 10m/s$ over a time period of ca. $2min$

measurements.

Acknowledgments

This work has been funded by the GreenTech Wind project, a collaboration of the EuroTech Universities. Measurement data are taken from the "Cross-Cutting Activities on Wind Turbine Noise" internal project at DTU Wind Energy.

References

[1] Megavind, 2016. Technological solutions to reduce the environmental impacts of wind-energy systems. Tech. rep., Megavind.
[2] Michelsen, J., 1992. "Basis3D-a platform for development of multiblock PDE solvers". *Technical University of Denmark, AFM,* ***92-05***.
[3] SØRENSEN, J. N., and Shen, W. Z., 2002. "Numerical modeling of wind turbine wakes". *Journal of fluids engineering,* ***124***(2), pp. 393–399.
[4] Ta Phuoc, L., 1994. "Modeles de sous maille appliques auxecoulements instationnaires decolles". In Proceedings of a DRET Conference: Aerodynamique Instationnare Turbulente-Aspects numeriques et experimentaux. Paris, France: DGA/DRET editors.
[5] Mann, J., 1998. "Wind field simulation". *Probabilistic Engineering Mechanics,* ***13***(4), oct, pp. 269–282.
[6] Shen, W. Z., Michelsen, J. A., and SØRENSEN, J. N., 2004. "A collocated grid finite volume method for aeroacoustic computations of low-speed flows". *Journal of Computational Physics,* ***196***(1), pp. 348–366.
[7] Brooks, T., Pope, D., and Marcolini, M., 1989. *Airfoil self-noise and prediction.*
[8] Lowson, M. V., 1993. *Assessment and Prediction of Wind Turbine Noise.* Harwell Laboratory, Energy Technology Support Unit.
[9] Zhu, W. J., Heilskov, N., Shen, W. Z., and SØRENSEN, J. N., 2005. "Modeling of Aerodynamically Generated Noise From Wind Turbines". *Journal of Solar Energy Engineering,* ***127***(4), p. 517.
[10] Zhu, W. J., Shen, W. Z., and Sørensen, J. N., 2016. "Improvement of airfoil trailing edge bluntness noise model". pp. 1–12.

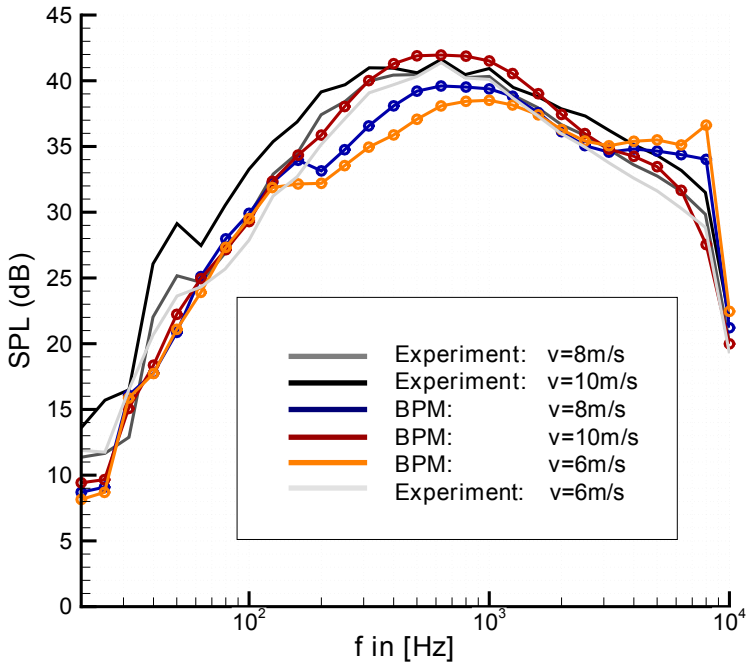

Figure 9. Comparison of A-weighted sound pressure level of semi empirical improved BPM calculations with measurements at $2.2R$ behind the turbine at wind speeds of $v = 6, 8, 10m/s$. Background noise has been added to semi empirical calculations

[11] Bertagnolio, F., Madsen, H., and Fischer, A. A Combined Aeroelastic-Aeroacoustic Model for Wind Turbine Noise: Validation and Analysis of Field Measurements.
[12] Www.kulak.com.pl/Wiatraki/pdf/nordtank500.pdf. No Title.